Supporting Information

ZIF-67-derived $NiCo_2O_4$@Co_2P/Ni_2P honeycomb nanosheets on carbon cloth for high-performance asymmetric supercapacitors

Wen-wei Song,[a] Bing Wang,[a] Xiao-man Cao,*[b] Qiang Chen,[a] and Zheng-bo Han*[a]

[a] *College of Chemistry, Liaoning University, Shenyang 110036, P. R. China E-mail: ceshzb@lnu.edu.cn*

[b] *College of Chemistry and Materials Engineering, Bohai University, Jinzhou 121013, P.R. China E-mail: caoxiaoman@bhu.edu.cn*

Summary

S1. Supporting experimental section.

S2. Supporting Figure S1~S11.

S3. Supporting Table S1.

Electrochemical Calculation

Capacitances of single electrode

The areal capacitance of a single electrode in three-electrode system can be calculated based on galvanostatic charge-discharge experiments according to equations:

$$C_S = \frac{I\Delta t}{S\Delta V} \quad (1)$$

Where C_s (F cm^{-2}) represents the areal capacitance, I is the discharge current (A), Δt represents the discharge time (s), S (cm^2) is the apparent area of actives materials loaded in working electrode, and ΔV is the potential window (V).

Capacitances of ASC devices

The volume specific capacitance of $NiCo_2O_4$@Co_2P/Ni_2P-CC//AC/CC devices can be calculated based on galvanostatic charge-discharge experiments according to equations:

$$C_V = \frac{I\Delta t}{V\Delta V} \quad (2)$$

Where C_v (F cm^{-3}) represents the volume specific capacitance, I is the discharge current (A), Δt represents the discharge time (s), V (cm^3) represents the apparent volume of actives materials loaded in working electrode and ΔV is the potential window (V).

In order to obtain more stable electrochemical performance, the positive and negative electrodes should follow the principle of equal capacitance. The relationship between positive and negative capacitance can be determined by the following equations equations:

$$Q = C_s \times \Delta V \times S \tag{3}$$

$$Q_+ = Q_- \tag{4}$$

$$\frac{C_{s,-}}{C_{s,+}} = \frac{S_+ \times \Delta V_+}{S_- \times \Delta V_-} \tag{5}$$

Where Q is the charge of the electrode, C_s represents the areal capacitance of the electrode, ΔV represents the potential window of the electrode, and S is the area of the electrode material. In this work, the active area of AC/CC and $NiCo_2O_4$@Co_2P/Ni_2P-CC was 1 cm^2. In addition, ΔV_-=1 V and ΔV_+=0.6 V. According to the calculation (5), the ratio of areal capacitance of AC/CC and $NiCo_2O_4$@Co_2P/Ni_2P-CC was 0.6. Therefore, the areal capacitance of AC/CC should be adjusted to 1729.13 mF cm^{-2} at a current density of 2 mA cm^{-2}.

The energy density (E, mWh cm^{-3}) and power density (P, mW cm^{-3}) are calculated by the following equations:

$$E = \frac{\int IVdt}{V_v} \tag{6}$$

$$P = \frac{E}{\Delta t} \tag{7}$$

Where V represents the potential window, V_V represents the volume of device and Δt represents the diacharge time.

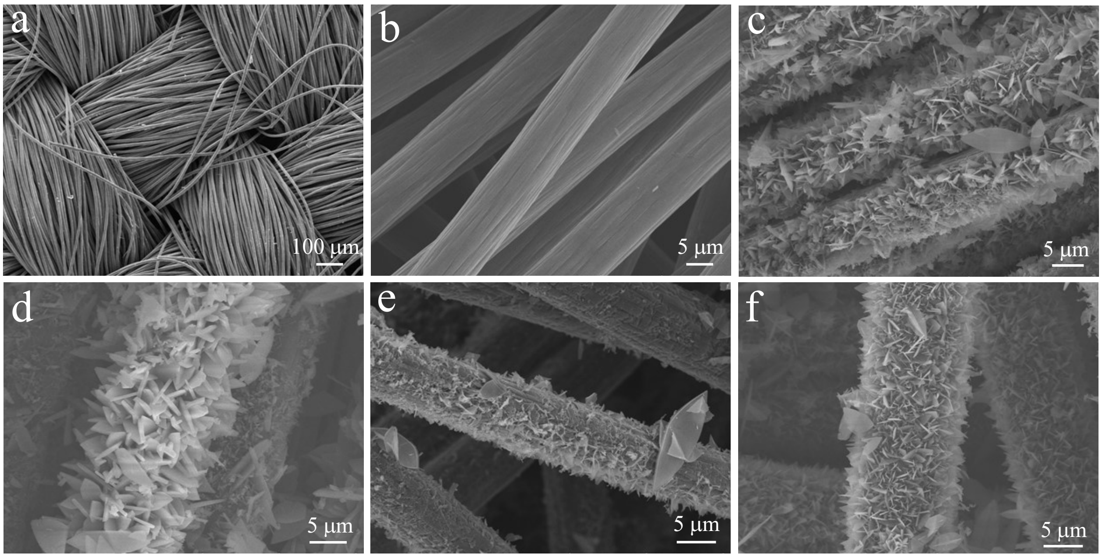

Figure S1. (a, b) SEM images of CC. (c) SEM images of ZIF-67-CC-Ⅰ. (d) SEM images of ZIF-67-CC-Ⅱ. (e) SEM images of ZIF-67-CC-Ⅲ. (f) SEM images of ZIF-67-CC-Ⅳ.

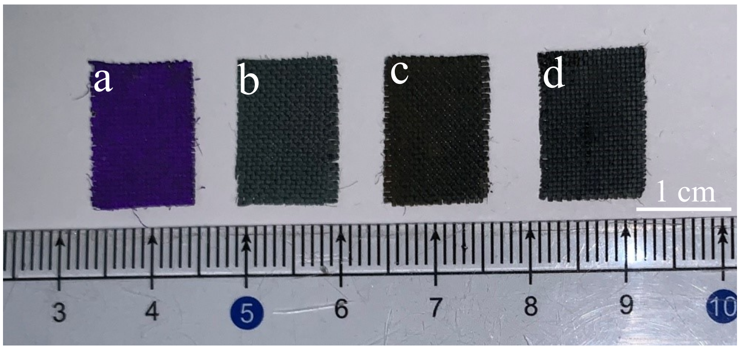

Figure S2. (a) Picture of ZIF-67-CC. (b) Picture of Co-Ni LDH-CC. (c) Picture of $NiCo_2O_4$-CC. (d) Picture of $NiCo_2O_4$@Co_2P/Ni_2P-CC.

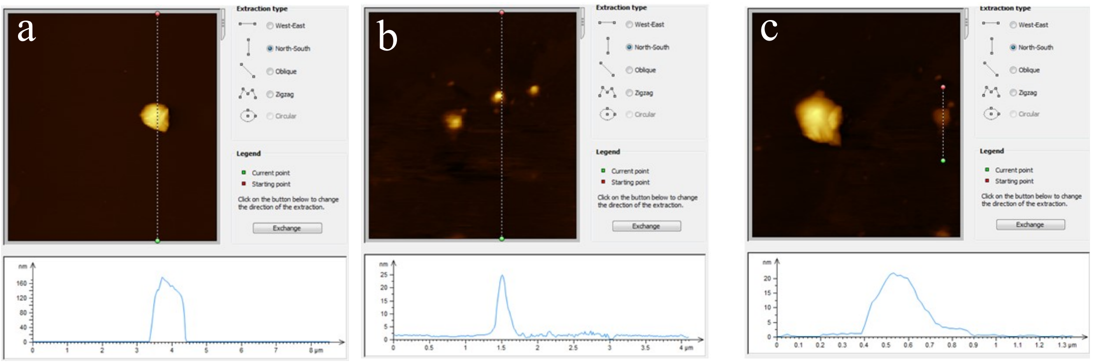

Figure S3. (a) AFM images of ZIF-67-CC. (b) AFM images of Co-Ni LDH-CC. (c) AFM images of $NiCo_2O_4$@Co_2P/Ni_2P-CC.

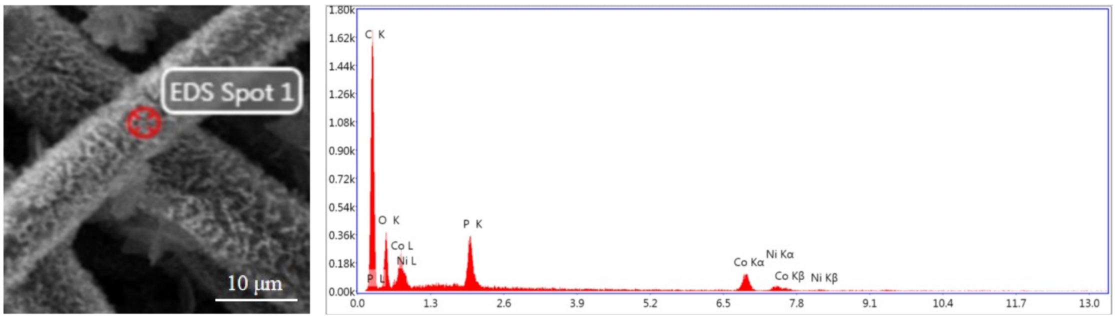

Figure S4. EDS point scan test results of $NiCo_2O_4$@Co_2P/Ni_2P-CC.

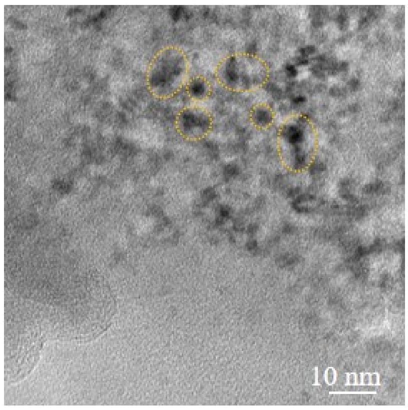

Figure S5. HRTEM images of $NiCo_2O_4$@Co_2P/Ni_2P-CC.

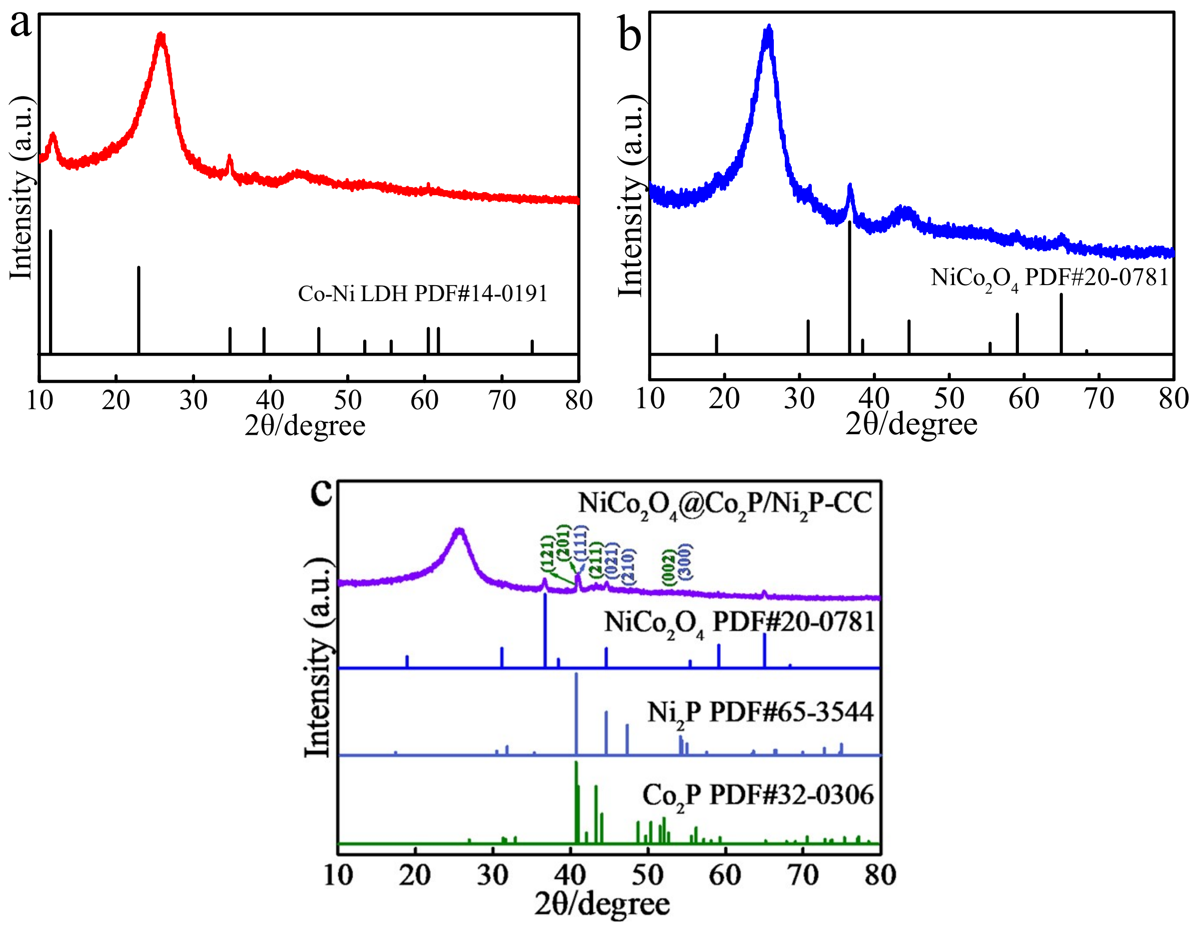

Figure S6. (a) PXRD patterns of Co-Ni LDH-CC. (b) PXRD patterns of $NiCo_2O_4$-CC. (c) PXRD patterns of $NiCo_2O_4$@Co_2P/Ni_2P-CC.

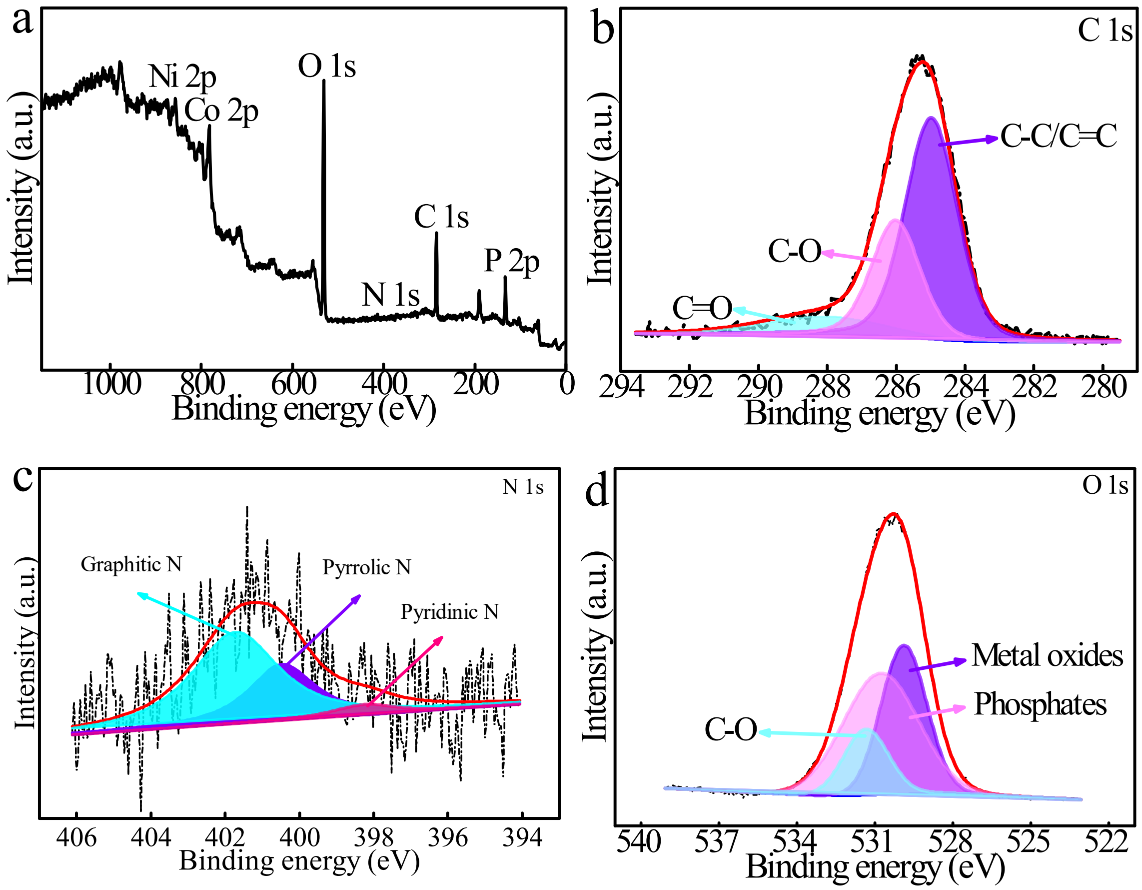

Figure S7. (a) Survey spectra of $NiCo_2O_4$@Co_2P/Ni_2P-CC. (b, c and d) C 1s, N 1s and O 1s high-resolution XPS spectra of $NiCo_2O_4$@Co_2P/Ni_2P-CC.

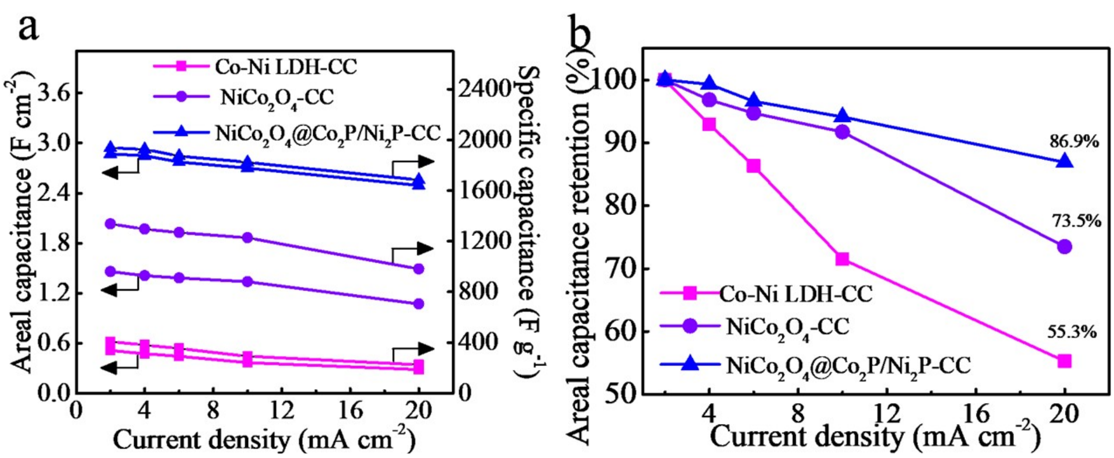

Figure S8. (a) The areal capacitance and specific capacitance of Co-Ni LDH-CC, $NiCo_2O_4$-CC and $NiCo_2O_4$@Co_2P/Ni_2P-CC at different current density from 2 to 20 mA cm^{-2}. (b) The areal capacitance retention of Co-Ni LDH-CC, $NiCo_2O_4$-CC and $NiCo_2O_4$@Co_2P/Ni_2P-CC at different current density from 2 to 20 mA cm^{-2}.

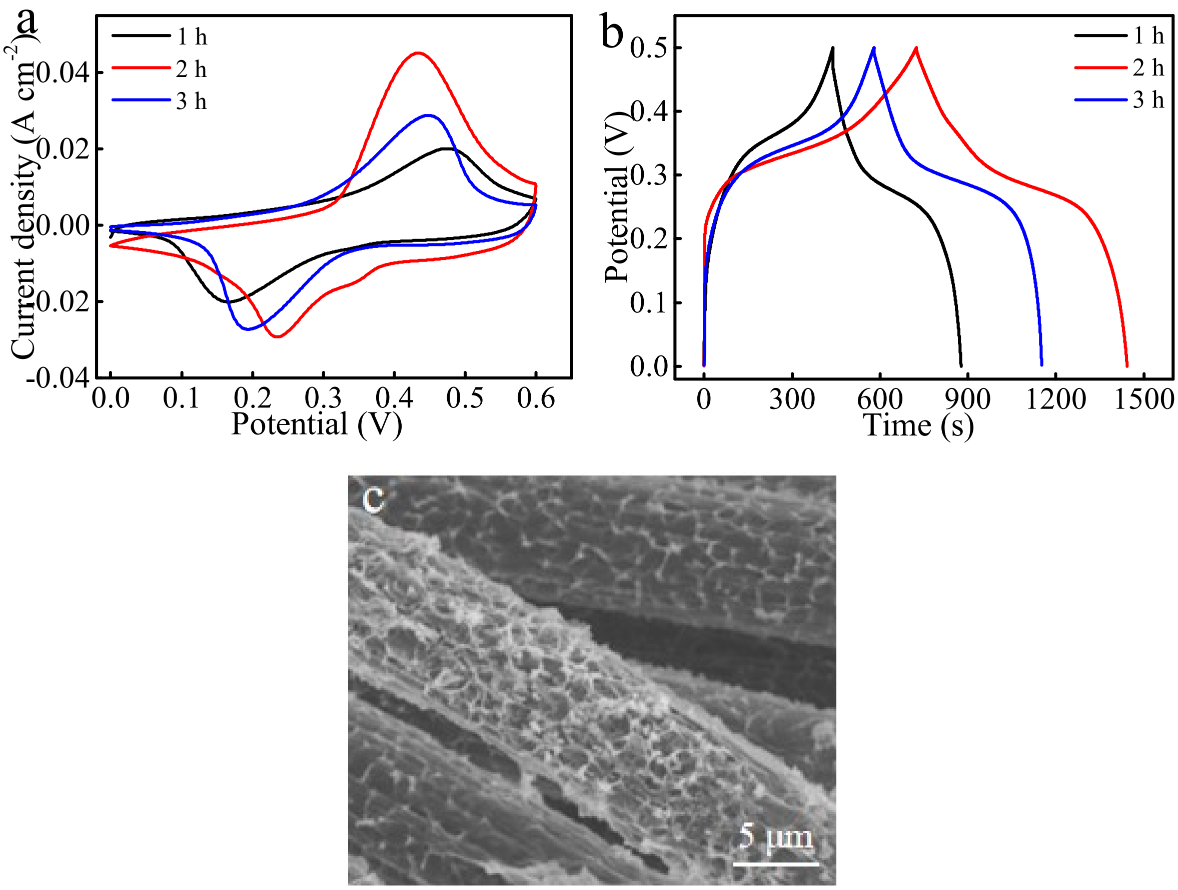

Figure S9. (a) CV curves of $NiCo_2O_4$@Co_2P/Ni_2P-CC on different phosphatization time from 1 h to 3 h at a scan rate of 10 mV s^{-1}. (b) GCD curves of $NiCo_2O_4$@Co_2P/Ni_2P-CC on different phosphatization time from 1 h to 3 h at a current density of 2 mA cm^{-2}. (c) SEM images of $NiCo_2O_4$@Co_2P/Ni_2P-CC on phosphatization time of 3 h.

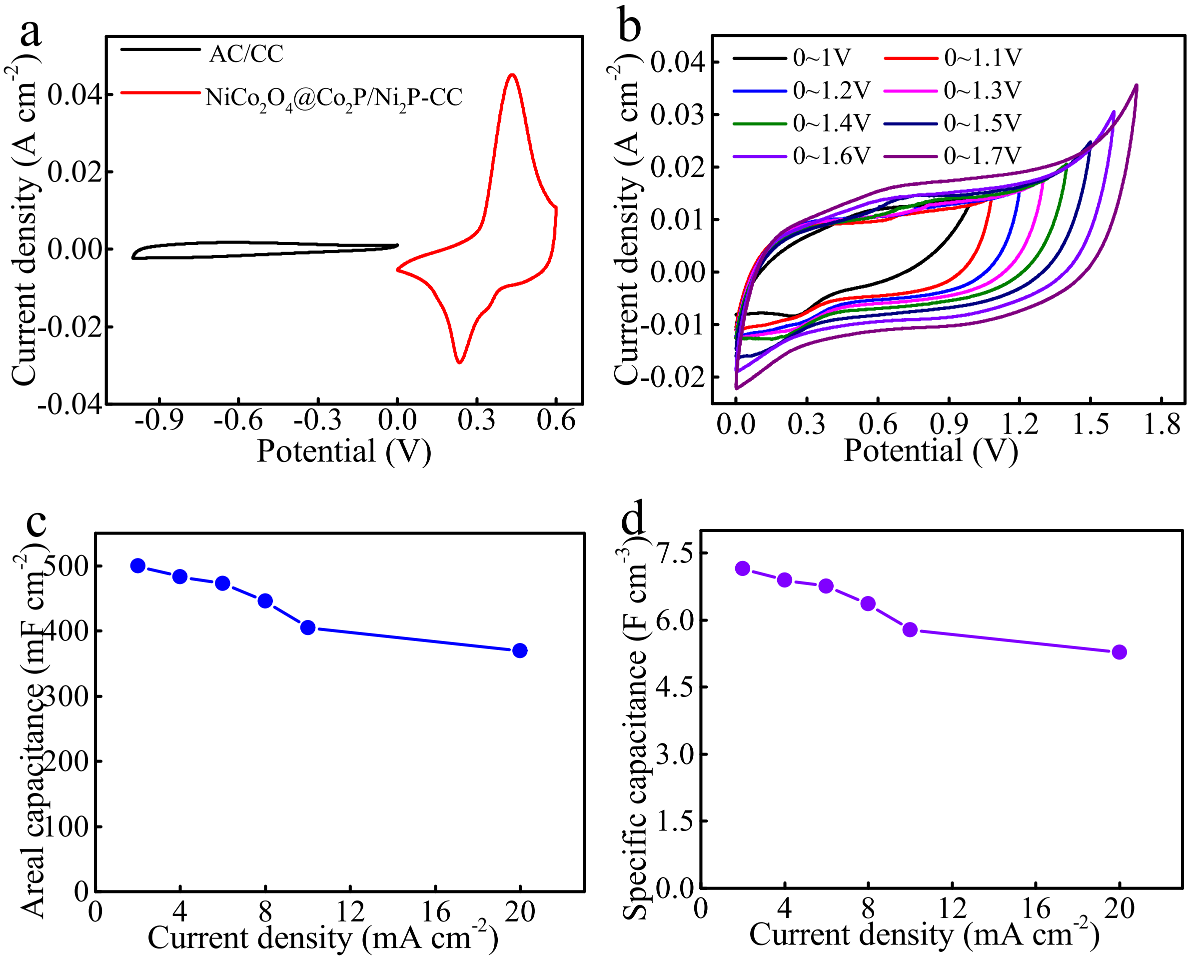

Figure S10. (a) CV curve of $NiCo_2O_4$@Co_2P/Ni_2P-CC and AC/CC at scan rate of 10 mV s^{-1}. (b) CV curves of $NiCo_2O_4$@Co_2P/Ni_2P-CC and AC/CC at different voltage window at a scan rate of 10 mV s^{-1}. (c) Areal capacitance of $NiCo_2O_4$@Co_2P/Ni_2P-CC/AC/CC at different current from 2 to 20 mA cm^{-2}. (d) Specific capacitance of $NiCo_2O_4$@Co_2P/Ni_2P-CC/AC/CC at different current density from 2 to 20 mA cm^{-2}.

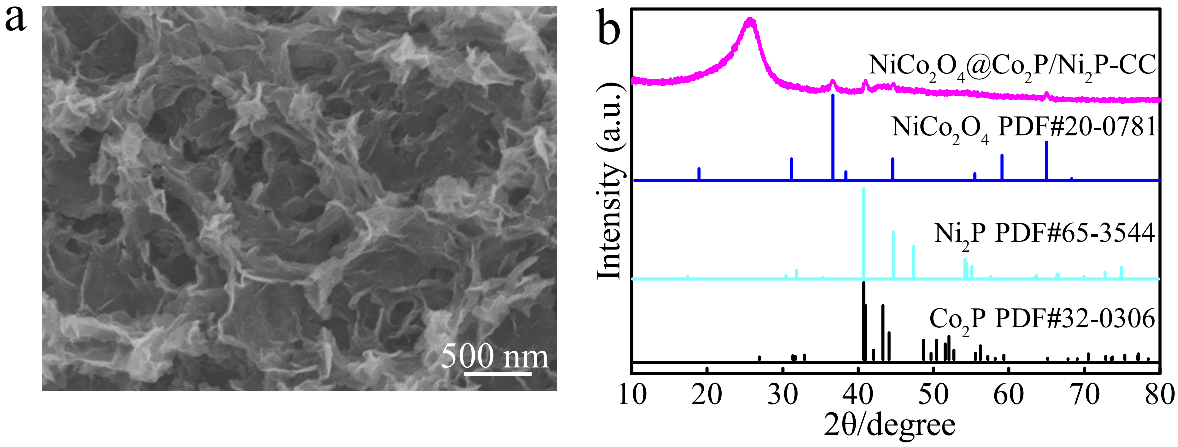

Figure S11. (a) SEM and (b) XRD images of $NiCo_2O_4$@Co_2P/Ni_2P-CC electrode material after 10000 cycles by charge-discharge cycle at 2 mA cm^{-2}.

Table S1. Comparison of $NiCo_2O_4@Co_2P/Ni_2P$-CC with various Ni/Co based electrodes materials for supercapacitor.

Type	Morphology	Electrolyte	Scan rate/ current density	Capancitance	Ref.
$CoO@MnO_2$	Nanosheets arrays	6 M KOH	2 mA cm^{-2}	2.4 F cm^{-2}	1
Zn-Ni-Co TOH	Nanowire array	1 M KOH	3 mA cm^{-2}	2.14 F cm^{-2}	2
$CoO/Co_9S_8@CN$	Nanocage cluster	6 M KOH	0.5 A g^{-1}	303.3 F g^{-1}	3
$Ni(OH)_2$	Nanosheets	6 M KOH	5 mA cm^{-2}	0.863 F cm^{-2}	4
Ni Co-LDH@Au-CuO/Cu	Array	3 M KOH	1.5 mA cm^{-2}	1.97 F cm^{-2}	5
NiNW@NiCo-DH/NF	Nanosheets @Nanowire	6 M KOH	5 mA cm^{-2}	2.25 F cm^{-2}	6
$NiCo_2O_4@MnO_2$	Nanosheets	1 M KOH	5 mA cm^{-2}	2.85 F cm^{-2}	7
Co-Ni LDH-CC	Honeycomb nanosheets	6 M KOH	2 mA cm^{-2}	0.512 F cm^{-2}	**This work**
$NiCo_2O_4$-CC	Honeycomb nanosheets	6 M KOH	2 mA cm^{-2}	1.458 F cm^{-2}	**This work**
$NiCo_2O_4@Co_2P/Ni_2P$-CC	Honeycomb nanosheets	6 M KOH	2 mA cm^{-2}	2.88 F cm^{-2}	**This work**

References

1 X. Z. Wang, Y. H. Xiao, D. C. Su, S. G. Xu, L. M. Zhou, S. D. Wu, L. F. Han, S. M. Fang, S. K. Cao, Hierarchical porous cobalt monoxide nanosheets@ultrathin manganese dioxide nanosheet core-shell arrays for high-performance asymmetric supercapacitor, *Int. J. Hydrogen Energy,* 2016, **41**, 13540-13548.

2 Z. H. Huang, F. F. Sun, M. Batmunkh, W. H. Li, H. Li, Y. Sun, Q. Zhao, X. Liu, T. Y. Ma, Zinc-nickel-cobalt ternary hydroxide nanoarrays for high-performance supercapacitors, *J. Mater. Chem. A,* 2019, **7**, 11826-11835.

3 C. Shi, M. W. Chen, X. Han, Y. F. Bi, L. L. Huang, K. Zhou, Z. P. Zheng, Thiacalix[4]arene-supported tetradecanuclear cobalt nanocage cluster as precursor to synthesize CoO/Co_9S_8@CN composite for supercapacitor application, *Inorg. Cherm. Front.,* 2018, **5**, 1329-1335.

4 X. Liu, Y. Yang, X. X. Xing, T. Zou, Z. D. Wang, Y. D. Wang, From water and Ni foam to a $Ni(OH)_2$@Ni foam binder-fFree supercapacitor electrode: a green corrosion route, *ChemElectroChem,* 2018, **5**, 434-444.

5 Y. Q. Guo, X. F. Hong, Y. Wang, Q. Li, J. S. Meng, R. T. Dai, X. Liu, L. He, L. Q. Mai, Multicomponent hierarchical Cu-doped NiCo-LDH/CuO double arrays for ultra-long life hybrid fiber supercapacitor, *Adv. Funct. Mater.,* 2019, **29**, 1809004.

6 L. Li, X. Liu, C. Liu, H. Z. Wan, J. Zhang, P. Liang, H. B. Wang, H. Wang, Ultra-long life nickel nanowires@nickel-cobalt hydroxide nanoarrays composite pseudocapacitive electrode: construction and activation mechanism, *Electrochim. Acta,* 2018, **259**, 303-312.

7 R. J. Zou, M. F. Yuen, Z. Y. Zhang, J. Q. Hu, W. J. Zhang, Three-dimensional networked $NiCo_2O_4/MnO_2$ branched nanowire heterostructure arrays on nickel foam with enhanced supercapacitor performance, *J. Mater. Chem. A,* 2015, **3**, 1717-1723.